PHYSICAL REVIEW B VOLUME 17, NUMBER 6 15 MARCH 1978

Surface energy bands and atomic position of Cl chemisorbed on cleaved Si(111)

P. K. Larsen
Philips Research Laboratories, Eindhoven, The Netherlands

N. V. Smith, M. Schlüter, and H. H. Farrell
Bell Laboratories, Murray Hill, New Jersey 07974

K. M. Ho and Marvin L. Cohen
Department of Physics, University of California, Berkeley, California 94720
and Materials and Molecular Research Division, Lawrence Berkeley Laboratory, Berkeley, California 94720

(Received 3 October 1977)

Angle-resolved photoemission measurements using synchrotron radiation have been performed on a cleaved Si(111) surface covered to saturation with Cl. Two main Cl-induced peaks, identified as the σ and π bonding levels, are observed, and the angular dependence of their intensities supports the onefold site for the Cl adatoms. The two-dimensional energy bands for the σ, π, and two previously unobserved levels, designated b and s, are mapped directly from the angular dependence of peak positions. As far as dispersion and rough energy location are concerned, these Cl-induced surface energy bands are in remarkably good agreement with self-consistent pseudopotential calculations. There are some minor differences in detail, concerning precise energy locations and band splittings. The b level is identified, on the basis of the pseudopotential charge densities, as a state involving the Si back-bonding orbitals. The s level is attributed to bonding between Cl p_z and Si s orbitals, in contrast to the σ level which involves bonding between Cl p_z and Si p_z orbitals.

I. INTRODUCTION

Angle-resolved photoemission is a technique which can be used to determine both the atomic and electronic structure of surfaces.[1] In this paper we report an angle-resolved photoemission study of Cl adsorbed on the cleaved Si(111) surface. Our measurements of the angular dependence of the intensities of Cl-induced features in the photoemission spectra lead to the conclusion that the Cl atoms sit in the onefold, or covalent, site—a result in agreement with the conclusions of other studies. From the angular dependence of peak positions in the spectra, we obtain energy (E) versus parallel wave vector ($k_\parallel$) dispersion relations for a number of the Cl-derived levels. Theoretical $E(k_\parallel)$ relations have been calculated for the covalent position using a pseudopotential method, and are found to bear a strong resemblance to the experimental $E(k_\parallel)$ curves. There are, however, some minor differences in details. The end product of our experimental and theoretical investigations, therefore, is a rather detailed picture of the chemical bonding of this particular surface system.

The format of this paper is as follows. In Sec. II, we describe the experimental details. Typical experimental results are shown and the atomic position of Cl on the Si(111) surface is discussed in Sec. III. In Sec. IV, we present and discuss the experimental Cl-induced surface energy bands. In the concluding Sec. V, the results of the pseudopotential calculation are presented and compared with our experimental results.

II. EXPERIMENTAL DETAILS

The angle-resolving photoemission spectrometer system used in these studies is described elsewhere,[2] and has two electron-energy analyzers of the plane-mirror type. All the measurements reported here were taken with only one of the analyzers, the one which samples photoelectrons propagating in the plane of incidence. The geometry of the experimental measuring system is shown schematically in Fig. 1. Monochromatic radiation was obtained from the ultra-high-vacuum Seya-Namioka beam line on the Tantalus I storage ring, located at the University of Wisconsin Synchrotron Radiation Center. The radiation was incident on the surface at 45° in a p-polarization configuration. The angular and energy resolutions

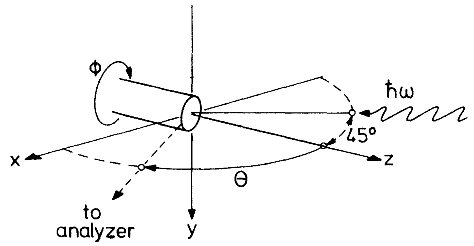

FIG. 1. Schematic diagram of the geometry of the experimental measuring system.

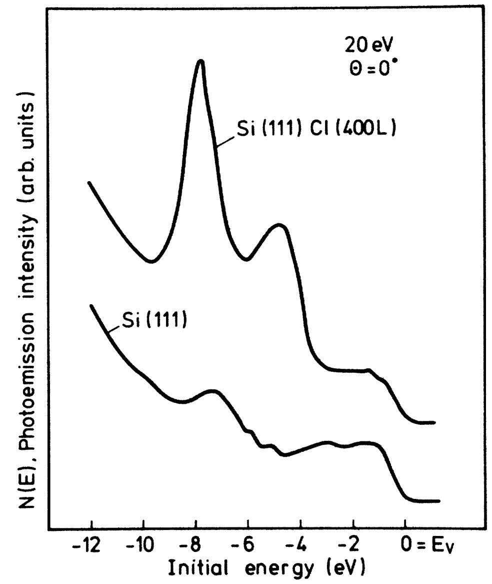

FIG. 2. Photoelectron-energy spectra taken at normal emission and $\hbar\omega = 20$ eV for a clean and chlorine-covered Si(111) surface.

are estimated to be ±2° and 0.4 eV, respectively.

The surfaces were prepared by cleaving single crystals of Si in an atmosphere of Cl_2. The pressure was 8×10^{-7} Torr and the total exposure was ~400 L (1 Langmuir = 10^{-6} Torr sec). Under these conditions, a saturation coverage of Cl with a $p(1 \times 1)$ structure is obtained.[3] After exposure, the Cl_2 gas was pumped away, and the photoemission measurements performed. Several cleaves were performed, and the results were found to be reproducible.

The effect of chlorine adsorption on the photoemission spectrum of Si(111) is illustrated in Fig. 2. These spectra were taken at normal emission ($\theta = 0°$) at the photon energy $\hbar\omega = 20$ eV, and are plotted against initial-state energy taking zero at the valence-band maximum E_V. Two very prominent Cl-induced peaks appear in the energy range -9 to -4 eV. The peak at the higher initial energy (lower binding energy) has been identified as due to the Cl $p_{x,y}$ or π-bonding orbital, and the peak at lower energy has been identified at the Cl p_z or σ-bonding orbital.[4] Our own identifications confirm these assignments, as will be discussed in Sec. III.

III. CHLORINE ATOMIC POSITION

There are two likely possibilities for the position of Cl atoms adsorbed on Si(111). The first is the onefold site where the Cl atom sits directly above a surface Si atom. The second is the threefold site where the Cl atom sits in the open space between three neighboring surface Si atoms. The two positions are indicated in Fig. 3. Two inequivalent threefold sites actually exist. However, they only differ from each other in second-nearest-neighbor positions. The theoretical calculations to be described below are performed on a structure with Cl sitting on top of a second-layer void. Pseudopotential calculations for the onefold geometry show that the Cl p_z orbital (the z axis is taken perpendicular to the surface) gives rise to a peak in the surface density of states at appreciably lower energies than the peak associated with the $p_{x,y}$ orbitals.[4] This is consistent with simple chemical intuition. In the onefold site the Cl p_z orbital will overlap with the Si dangling orbital and form a covalent bond of σ symmetry having an energy lower than that of the $p_{x,y}$ orbitals. The onefold site is therefore sometimes referred to as the covalent site. On the other hand, similar calculations for the threefold site show that the p_z orbital is less strongly bound than the $p_{x,y}$ orbitals but is not well resolved from them. This is again consistent with chemical intuition for this more ionic site.

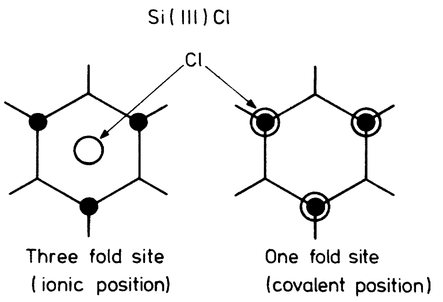

FIG. 3. Possible atomic positions of chlorine adsorbed on a silicon (111) surface.

The observation that the Cl-induced contribution to the photoemission spectrum consists of two well-resolved major peaks, as in Fig. 2, immediately favors the onefold or covalent site. As further confirmation, Schlüter *et al.*[4] show that the observed dependence of the lower energy peak on the polarization of the incident radiation is, under certain simplifying assumptions, consistent with σ symmetry. We show now that the same assignment can be arrived at independently from the angular dependence of the two major peaks.

Figure 4 shows the photoelectron energy spectra of Cl on Si(111) as a function of polar angle θ. These data were taken at $\hbar\omega = 24$ eV in the $\Gamma M \Gamma$ azimuth. It is noted that the intensities of the two main peaks vary strongly with θ. There are also changes in peak positions, but discussion of these changes is deferred until Sec. IV. The intensity

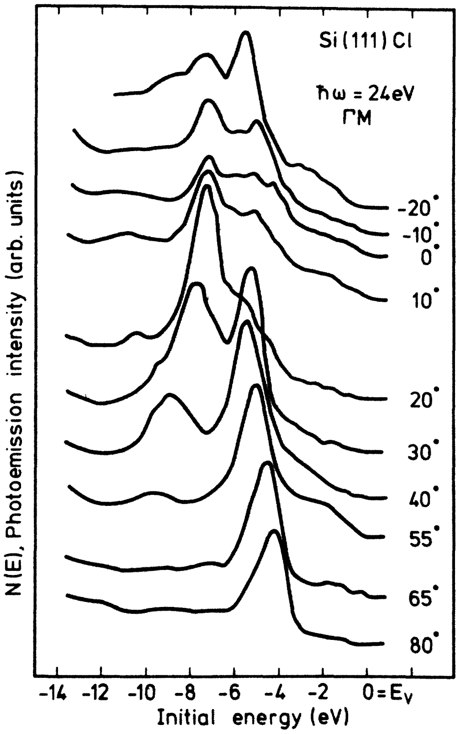

FIG. 4. Polar-angle dependence of the spectra for Cl on Si(111) taken at $\hbar\omega = 24$ eV along the $\Gamma M \Gamma$ azimuth.

variations of the two main peaks are plotted against θ in Fig. 5. What is plotted here is actually the normalized peak intensity, i.e., peak height divided by $\cos\theta$. The cosine factor accounts for the particular experimental geometry used here, in which the area of the sample "seen" by the analyzer is larger than the area actually illuminated. (The opposite situation would be the so-called "flooded-source" configuration in which the illuminated area is always larger than the area seen by the detector.) Inclusion of the $\cos\theta$ factor, however, is partly for "cosmetic" purposes, and our qualitative conclusions do not depend on whether this factor is included or not. The normalized intensity of the Cl-induced peak at lowest initial state energy is represented by the dashed curve in Figure 5. There is a well-defined maximum in the range $\theta = 20° - 25°$. The corresponding results for the other main peak (full curve in Fig. 5) show a main maximum near $\theta = 70°$, and a local minimum near $\theta = 0°$.

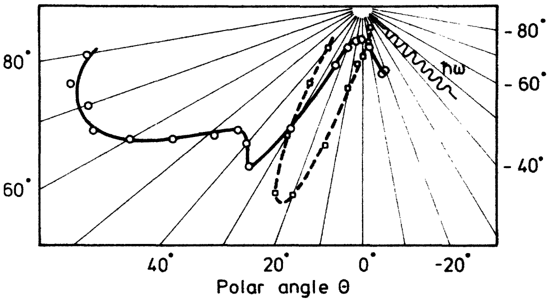

FIG. 5. Plots of the θ dependence of the intensities of the two main Cl-induced peaks in the $\Gamma M \Gamma$ azimuth. The full (dashed) curve corresponds to the higher (lower) initial-energy peak in the data of Fig. 4.

These results can be understood qualitatively in terms of the simple model of Gadzuk.[5] This is a model which is known to be inexact. However, there are indications from both x-ray[6,7] and ultraviolet experiments[8] that the model may be of use in making qualitative identifications of orbital character. In the Gadzuk model, it is assumed that the wave function of the final state in the optical transition which gives rise to the photoelectron may be adequately represented by a single plane wave of momentum $\vec{p}$; $|f\rangle = e^{i\vec{p}\cdot\vec{r}}$. The initial state is represented as an oriented atomic orbital; $|i\rangle = \psi(\vec{r})$. The intensity of emission of photoelectrons with momentum $\vec{p}$ from the orbital $\psi(\vec{r})$ is then given by

$$I(\vec{p}) \propto (\vec{A}\cdot\vec{p})^2 \, |\tilde{\psi}(\vec{p})|^2 \,, \tag{1}$$

where $\vec{A}$ is the vector potential of the electromagnetic field, and $\tilde{\psi}$ is the Fourier transform, or momentum representation, of the orbital ψ. The angular dependence of an atomic orbital is the same in both real space and momentum space. The other main angular dependence is embodied in the $(\vec{A}\cdot\vec{p})^2$ term and is determined by the polarization of the incident radiation. These various factors are illustrated schematically in Fig. 6. The radiation is incident at 45°, so that $(\vec{A}\cdot\vec{p})^2$ gives rise to a $\cos^2$ distribution as shown. (Strictly speaking, we should take into account the reflected and transmitted electromagnetic waves as well. These considerations, and also the complications associated with surface local field effects,[9] are ignored here.) The angular dependence of $|\tilde{\psi}(\vec{p})|^2$ for p_z and p_x orbitals are also shown as dashed curves in the lower half of Fig. 6. Multiplication of these curves with the $(\vec{A}\cdot\vec{p})^2$ factor gives rise to the full curves, whose lobes have their maxima at $\theta = 22.5°$ and 67.5° for the p_z and p_x orbitals, respectively. In this model the p_y orbitals are invisible since the electron-energy analyzer lies always in the nodal plane of this orbital.

Comparison of the data of Fig. 5 with the simple model results of Fig. 6 leads us to identify the Cl-induced peak at lower (higher) initial state energy with the Cl p_z ($p_{x,y}$) orbitals. This identification immediately leads to the onefold (or covalent)

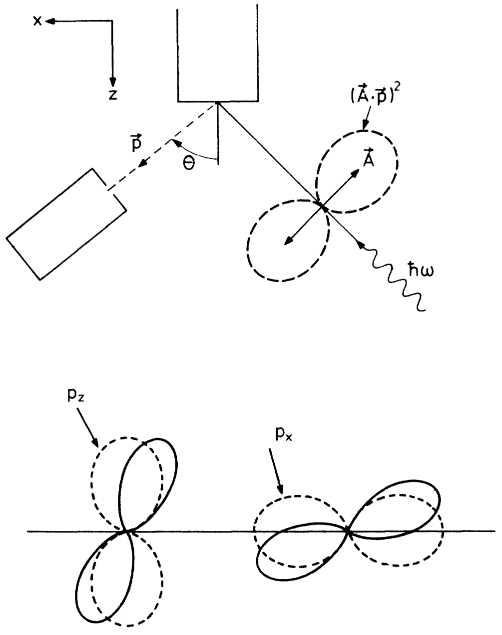

FIG. 6. Schematic representation of the angular dependences of $(\vec{A}\cdot\vec{p})^2$ and $|\tilde{\psi}(\vec{p})|^2$ for p_x and p_z orbitals (dashed curves). Full curves represent the product $(\vec{A}\cdot\vec{p})^2|\psi(\vec{p})|^2$.

choice for the Cl atomic position. This conclusion agrees with the earlier conclusions of Schlüter *et al*,[4] based on a combined theoretical and experimental approach to the polarization dependence of the angle-integrated photoemission. We wish to emphasize, however, that our present assignment of the Cl atomic position can be made independently of the earlier theoretical and experimental work. Using angular considerations alone, we identify the lower energy peak as Cl p_z derived. Using the chemical intuition considerations discussed above, we are then automatically led to the onefold site geometry.

It should be noted that the π emission identified with Cl $p_{x,y}$ orbitals in Fig. 5 (full curve) exhibits a relative maximum at about $\theta = 35°$, which is not accounted for by the simple model described above. This maximum is due to emission from states involving Si back-bonding orbitals in addition to the π emission, i.e., at $\theta \sim 35°$ there is a partial energy overlap of these different initial states. We shall discuss this point further below.

IV. SURFACE ENERGY BANDS

In addition to the intensity variation discussed above, it is found that the energy positions of Cl-induced peaks vary with angle. This effect can be seen in Fig. 7, which shows a sequence of spectra taken at various polar angles in the ΓKM azimuth

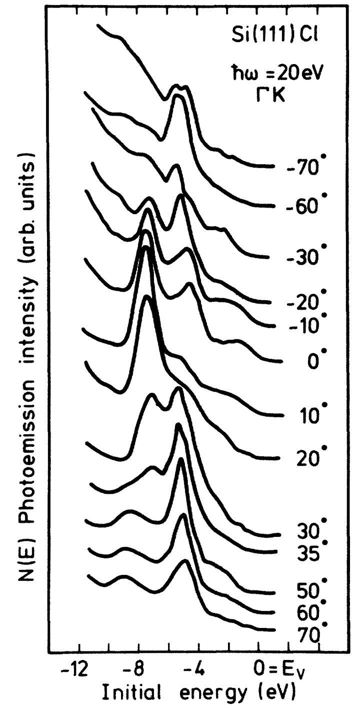

FIG. 7. Polar-angle dependence of the spectra for Cl on Si(111) taken at $\hbar\omega = 20$ eV along the ΓKM azimuth.

at $\hbar\omega = 20$ eV. From these results we have derived the two-dimensional energy bands by the usual procedure. For each peak we read the kinetic energy T in vacuum and then obtain the parallel wave vector, $k_\parallel$ by applying the elementary formula

$$k_\parallel = (2mT/\hbar^2)^{1/2}\sin\theta\,. \tag{2}$$

Each peak therefore gives rise to a point in an E vs $k_\parallel$ plot, and the results corresponding to the spectra in Fig. 7 are shown in Fig. 8. The data refer to initial state energy $E \equiv T - \hbar\omega + \xi$, where ξ is the ionization potential. Positive values of $k_\parallel$ correspond to emission projecting on the $[0\bar{1}1]$ direction. Points having negative values of $k_\parallel$ were obtained at negative polar angles or after a 180° rotation of the sample about its normal at positive polar angles.

Smooth curves have been drawn through the experimental points of Fig. 8. These curves were drawn subject to two constraints: (a) the curve must be symmetrical about Γ, i.e., $E(k_\parallel) = E(-k_\parallel)$ and (b) the energies at the M point must be consistent with those at the M point along the $\Gamma M \Gamma$ azimuth. This latter consideration, which will be discussed below, leads us to draw the main π band through the lower of the two sets of points at M. It is seen that the π band (based on the Cl $p_{x,y}$ orbitals) displays a considerable amount of dispersion. The π band has its maximum at an energy

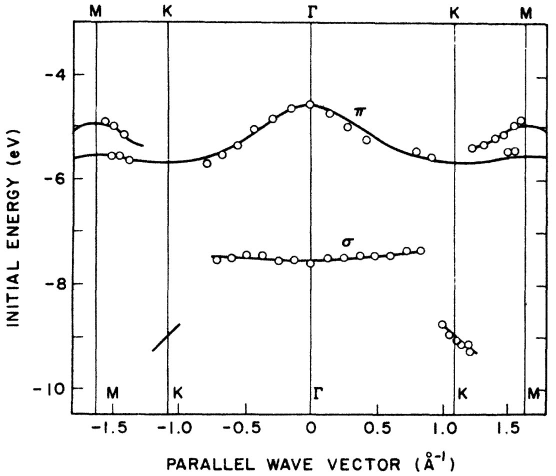

FIG. 8. Surface energy-band structure along Γ*KM* derived from the energy locations of Cl-induced features in the spectra of Fig. 7. Smooth curves have been drawn to pass near the experimental points and have the required symmetry.

of about −4.5 eV, and has its minimum near or at the zone boundary at an energy of about −5.7 eV. The σ band (based on the Cl p_z orbitals), on the other hand, is quite flat, appearing consistently at an energy of about −7.5 eV. It should be recognized that the numbers quoted above represent the positions of the maxima of peaks which have an appreciable width as is evident from an inspection of Figs. 2, 4, and 7.

In addition to the main π and σ bands, other features are observed in specific parts of the zone. Near the *M* point there is a band at about −5 eV, and near the *K* point there is a band in the range −9.4 to −8.7 eV. These will be identified with features in the pseudopotential calculations to be discussed in Sec. V.

The two-dimensional Brillouin zone appropriate to the unreconstructed surface of Si(111) is shown in Fig. 9. It is seen that if we vary $k_{\parallel}$ along the Γ*M*Γ azimuth, we expect the experimental bands to have mirror symmetry about the *M* point. We also expect the energies at the *M* point along the Γ*M*Γ azimuth to be the same as those obtained at the *M* point along the Γ*KM* azimuth. Earlier experiments on the layer compound InSe, which has the same two-dimensional Brillouin zone, showed that these symmetry requirements were strictly observed in the experimental data.[10]

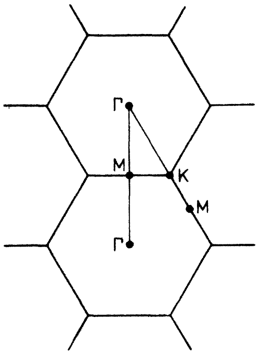

FIG. 9. Two-dimensional Brillouin zone appropriate to the 1×1 Si(111) surface.

Our experimental results for the Cl-derived energy bands in the Γ*M*Γ azimuth are shown in Fig. 10. These data were obtained from the spectra of Fig. 4 taken at $\hbar\omega = 24$ eV, augmented by additional spectra taken at $\hbar\omega = 19$ eV (not shown). Positive values of $k_{\parallel}$ correspond here to emission projecting on the $[\bar{1}\bar{1}2]$ direction. It is seen that the data are consistent with the requirement that $E(k_{\parallel}) = E(-k_{\parallel})$ and that the expected mirror symmetry about the *M* point is clearly displayed. Smooth curves embodying these symmetry properties exactly have been drawn close to the experimental points. The π peak is occasionally seen as a weakly resolved doublet, and so two π bands have been drawn. The higher of these passes through the *M* point at an energy of −5.6 eV. This band is therefore identified with the lower of the two bands found at *M* along the Γ*KM* azimuth. This is also the reason why the π band in Fig. 8 was drawn through the lower rather than higher sets of points, as mentioned above. The higher set of points at *M* along Γ*KM* are associated with the feature "*b*" found along Γ*M*Γ and shown in Fig. 10. This feature corresponds to a rather weak structure observed in the spectra taken at $\hbar\omega = 19$ eV. The smooth curve through these data points has been drawn dashed to indicate that its precise shape is more tentative than for the other structures.

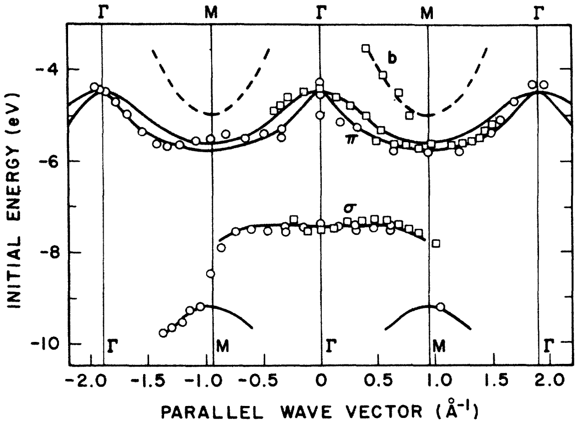

FIG. 10. Surface-energy band structure along Γ*M*Γ derived from the data of Fig. 4 (open circles) and additional spectra taken at $\hbar\omega = 19$ eV (open squares). Smooth curves have been drawn to pass near the experimental points, to have the required symmetry, and to be compatible with the data taken along the Γ*KM* azimuth.

Apart from this feature *b* the basic behavior for the $\Gamma M \Gamma$ azimuth is similar to that for the $\Gamma K M$ azimuth. The π band displays considerable downward dispersion away from Γ, whereas the σ band is quite flat. Below the σ band, a feature is observed in the energy range -10 to -9 eV, in the vicinity of the zone boundary.

V. PSEUDOPOTENTIAL CALCULATIONS

The electronic structure of Cl adsorbed on Si(111) has been calculated theoretically for both the onefold and threefold sites. The method is described in detail elsewhere.[11] Very briefly, it consists of setting up a pseudopotential Hamiltonian for a fictitious atomic structure composed of a sequence of thin films of material separated by thin regions of empty space. The system therefore retains a periodicity in the direction perpendicular to the films, so that standard pseudopotential methods can be applied, albeit with a rather large unit cell. The method is quite versatile and has been applied to the study of surface relaxation, reconstruction, and chemisorption.[12] The results for the surface density of states of Cl on Si(111) have been published earlier.[4]

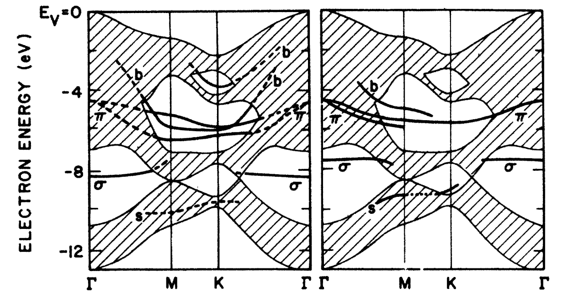

FIG. 11. Comparison between the results of pseudopotential calculations (left-hand panel) and a composite of the experimentally determined Cl-induced surface energy bands (right-hand panel). In each panel, the surface bands have been superimposed on the two-dimensional projection (represented by the cross-hatched regions) of the bulk Si energy band structure.

The calculated energy bands for Cl adsorbed in the onefold site on Si(111) are shown in the left-hand panel of Fig. 11. The cross-hatched regions

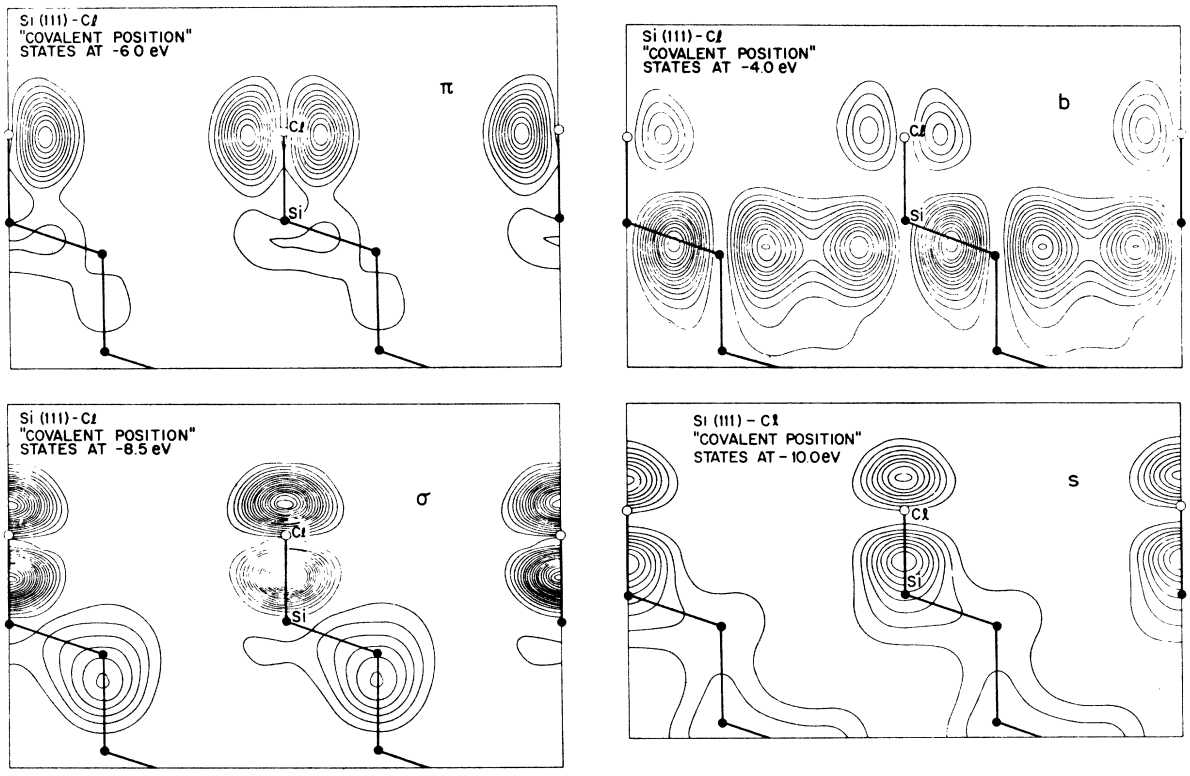

FIG. 12. Theoretical charge-density contour maps for the Cl-induced levels of the Si(111) Cl chemisorption system. The contours are displayed in a (110) plane intersecting the (111) surface at a right angle. The left-hand panel shows the maps for π-like (top) and σ-like (bottom) surface states; the right-hand panel shows the maps for Si back-bonding-like (top) and Si(s), Cl(p_z) bonding-like (bottom) surface resonances. The energy bands corresponding to these states are labeled π, σ, b, and s in Fig. 11.

represent the projection of the bulk Si band structure on the surface Brillouin zone. The full and dashed curves represent the Cl-induced energy bands. The σ band occurs for the most part in an absolute gap of the bulk Si band structure, and is therefore to be thought of as a true Cl surface state. The other bands, including the π bands, are degenerate with bulk Si states over parts of the zone, and are therefore to be thought of more as Cl surface resonances in these regions.

The right-hand panel of Fig. 11 represents a composite of our experimental results for the Cl-induced energy bands, superimposed on the same two-dimensional projection of the bulk Si band structure. It is seen that there is a remarkable overall similarity between the theoretical and experimental bands. In particular, the π band is predicted to be a doublet with downward dispersion away from Γ. The σ band, on the other hand, is predicted to be quite flat. The experimental features *b* and *s* also have their counterparts in the theoretical calculations, and will be discussed in more detail below.

Although the overall agreement is excellent, it is seen that there are some differences in detail. For example, although the maximum of the π bands occurs at -4.5 eV in both theory and experiment, the σ band occurs at -7.5 eV in experiment but at about -8.3 eV in theory. This discrepancy is probably related to the magnitude of the Cl pseudopotential. The present calculations are known to place the Cl 3*s* core level at too low an energy, suggesting that the Cl pseudopotential is too strong. Weakening of the Cl pseudopotential could raise the 3*s* core level and would have the effect of narrowing the σ-π separation. The anticipated correction is therefore in the correct sense to remove this discrepancy. We also note that the splitting between the two π bands is quite appreciable in the theoretical calculations. The splitting observed experimentally is small or is not well resolved. Also, it should be mentioned that because of finite resolution, the detailed connectivity of the π and *b* bands in the experimental part of Fig. 11 has been drawn in somewhat conjecturally.

The different nature of the π and σ levels is illustrated in Fig. 12, where theoretical charge density contours are displayed in a (110) plane cutting the (111) surface at a right angle. The surface localization and molecular character of these levels are readily observable. The peak designated σ is seen to be strongly Cl p_z-like, whereas the π peak is clearly $p_{x,y}$-like.

The real-space charge distributions calculated for the two other features labeled *b* and *s* are also presented in Fig. 12. Inspection of the charge distribution associated with the *b* bands shows that these states involve transverse (or back-bonding) orbitals between the first and second Si atomic layers. These states are modified by Cl chemisorption, but retain their primarily back-bonding character. Experimentally, the *b*-band features are rather weak, which probably explains why we missed most of the *b* bands predicted theoretically. However, as mentioned in Sec. III, a relative maximum in the intensity of the π emission is observed near $\theta = 35°$. At this polar angle $k_{\parallel} \sim 1.0\,\text{Å}$, i.e., the relative maximum is observed near the *M* point where the *b* bands exhibit a minimum and partly may overlap with the π bands. The intensity of this relative maximum depends on the direction of emission. This is observed in Fig. 13 where the intensity variation of the π emission is plotted against θ at $\hbar\omega = 24$ and 19 eV. The dashed (full) curves represent the intensity along (antiparallel to) the azimuth corresponding to the direction of the back-bond when going from the first to the second Si atomic layer. The difference in the charge density of the *b* states along these two azimuth seems to be the most probable cause of the differences in the emission intensity. Figure 13 also indicates that the (relative) emission intensity from the *b* bands and the π bands depends strongly on the photon energy. In order to separate the emission from these bands, it would be certainly worthwhile to repeat these experiments more

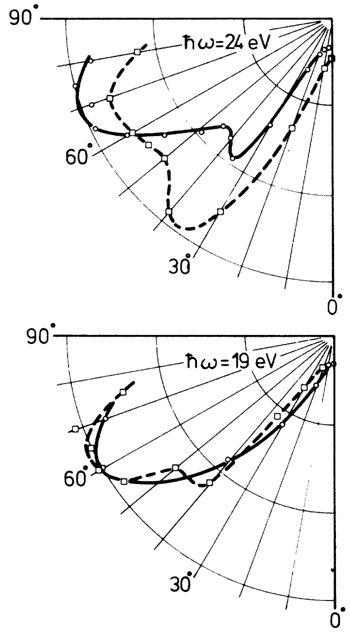

FIG. 13. Plots of the θ dependence of the intensity of the π-like peak in the $\Gamma M \Gamma$ azimuth at $\hbar\omega = 24$ and 19 eV. The dashed (full) curves correspond to emission with $\vec{k}_{\parallel}$ parallel to the $[\bar{1}\bar{1}2]$ direction ($[11\bar{2}]$ direction).

carefully under conditions of higher angular and energy resolution, at a number of photon-energies.

The low-energy s states correspond, according to the pseudopotential calculations illustrated in Fig. 12, to bonding between the Cl p_z and Si s orbitals. Our experimental results place this band almost 1 eV higher in energy than in the theoretical calculations. Indeed, the experimental band in the vicinity of the K point falls in the absolute gap of the Si bulk band structure, and is therefore a true surface state in this region, as opposed to a surface resonance in the calculations. Again, the discrepancy is probably related to the magnitude of the chlorine pseudopotential.

In summary, these angle-resolved photoemission studies have yielded information on the atomic position of Cl adsorbed on Si(111). In addition we have obtained, through comparison of theoretical and experimental $E(k_{\parallel})$ dispersion relations, a rather detailed picture of the chemical binding of this particular chemisorption system.

ACKNOWLEDGMENTS

We thank J. E. Rowe for a number of stimulating conversations. The help of A. H. Goemans in determining the crystallographic orientation of the sample is gratefully acknowledged. We are grateful also to E. M. Rowe, R. A. Otte, and other members of the University of Wisconsin Synchrotron Radiation Center for their friendly hospitality and help. The Tantalus I storage ring is supported by NSF Grant No. DMR-74-15089. Research for two of us (K.M.H. and M.L.C.) was supported in part by NSF Grant No. DMR 76-20647.

---

[1] As a general introduction to this topic, see *Photoemission and the Electronic Properties of Surfaces*, edited by B. Feuerbacher, B. Fitton, and R. F. Willis (Wiley, New York, to be published).

[2] N. V. Smith, P. K. Larsen, and M. M. Traum, Rev. Sci. Instrum. 48, 454 (1977).

[3] J. E. Rowe, Phys. Rev. Lett. 34, 398 (1975).

[4] M. Schlüter, J. E. Rowe, G. Margaritondo, K. M. Ho, and M. L. Cohen, Phys. Rev. Lett. 37, 1632 (1976).

[5] J. W. Gadzuk, Phys. Rev. B 10, 5030 (1974).

[6] R. H. Williams, P. C. Kemeny, and L. Ley, Solid State Commun. 19, 495 (1976).

[7] P. S. Wehner, J. Stöhr, G. Apai, F. R. McFeely, and D. A. Shirley, Phys. Rev. Lett. 38, 169 (1977).

[8] N. V. Smith and M. M. Traum, Phys. Rev. B 11, 2087 (1975); M. M. Traum, N. V. Smith, and F. J. DiSalvo, Phys. Rev. Lett. 32, 1241 (1974).

[9] J. G. Endriz, Phys. Rev. B 7, 3464 (1973); S. P. Weeks, and E. W. Plummer, Solid State Commun. 21, 695 (1977).

[10] P. K. Larsen, S. Chiang, and N. V. Smith, Phys. Rev. B 15, 3200 (1977).

[11] M. Schlüter, J. R. Chelikowsky, S. G. Louie, and M. L. Cohen, Phys. Rev. B 12, 4200 (1975).

[12] M. Schlüter, in *Proceedings of the Thirteenth International Conference on Physics of Semiconductors*, edited by F. G. Fumi (North-Holland, Amsterdam, 1976), p. 646.